ACS APPLIED MATERIALS & INTERFACES

Research Article

www.acsami.org

Monodispersed N-Doped Carbon Nanospheres for Supercapacitor Application

Whon-hee Lee and Jun Hyuk Moon*

Department of Chemical and Biomolecular Engineering, Sogang University, Seoul 121-742, Republic of Korea

Supporting Information

ABSTRACT: Highly monodispersed nitrogen-doped carbon nanospheres are prepared by the pyrolytic carbonization of emulsion-polymerized polystyrene-based colloidal spheres in the presence of a nitrogen-enriched molecule, melamine (1,3,5-triazine-2,4,6-triamine). The nitrogen-doped carbon spheres are successfully tested for use as electrode materials in supercapacitors. The nitrogen content incorporated into the carbon sphere is controlled by changing the weight ratio of melamine to the polymer spheres. The nitrogen doping concentration is proportional to the mixing weight ratio. The nitrogen doping produces relatively abundant pyridinic and pyrrolic configurations, and these configurations are observed to be more abundant for carbon spheres with high nitrogen doping. The nitrogen doping enhances the pseudocapacitance and the electrical conductivity of carbon, thereby enhancing the specific capacitance. We obtain a specific capacitance of up to 191.9 F g^{-1} with 20% nitrogen doped carbon nanospheres, which is 14 times higher than that of the undoped carbon nanospheres. Moreover, the capacitance retention remains up to 10 000 cycles, which clearly displays a good cycling stability the nitrogen-doped carbon nanospheres as the supercapacitve electrode materials.

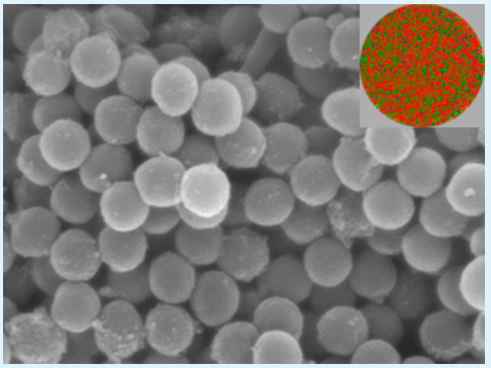

KEYWORDS: *carbons, carbon spheres, electrodes, nitrogen doping, supercapacitors, pseudocapacitances*

INTRODUCTION

Electrochemical capacitors or supercapacitors present an attractive new technology, specifically for high power applications such as hybrid electric vehicles or portable devices.[1,2] A supercapacitor stores electric energy by the physical adsorption of electrolyte ions onto a charged electrode by electrostatic attraction, resulting in the formation of a so-called electrochemical double layer (EDL).[3] Thus, to obtain high capacitance, large specific area materials such as porous materials have traditionally been preferred. Along with commercial activated carbon, synthetic porous carbons such as templated mesoporous carbons as well as various carbon allotropes such as carbon nanotubes (CNTs) and graphenes have been previously studied.[4−6]

This method of increasing the electric capacitance by increasing the surface area, that is, porosity, has a limitation, as this approach concurrently increases the material's electrical resistance, which lowers its potential to capture electrolyte ions.[7] Moreover, an increase in porosity increases the pore tortuosity, which impairs electrolyte ion transport.[8] There have thus been several experimental attempts to introduce metal oxides (e.g., RuO_2, MnO_2, and $Ni(OH)_2$) or conducting polymers (e.g., polyaniline, polypyrrole, and polythiophene).[9−12] In these cases, the electric charges could be stored by a direct charge transferred across the surface (i.e., Faradaic reaction), which is known as pseudocapacitance. More recently, as an alternative method, the introduction of heteroatoms (e.g., B, N, P and S) into carbon materials has been demonstrated as a facile and effective approach to enhance the capacitance.[6,12] Besides affecting the pseudocapacitance, the doping controls the semiconductor properties of carbon materials as well as their surface adsorption properties. Among these heteroatoms, nitrogen incorporation has received much attention. This may be because the doping can be achieved by either gas or solid precursors, and synergistic effects can be induced by the nitrogen doping. Nitrogen doping has been found to cause an increase in electric conductivity, and concurrently ameliorate surface wettability as well as adsorption properties that facilitate an electrochemical reaction on the carbon surface.[13−15] Various carbon morphologies including mesoporous carbons, CNTs, carbon nanofibers, and recently graphenes have been treated with nitrogen doping and tested as supercapacitors.[6,12,16−20]

In this paper, we have, for the first time, prepared highly monodispersed, nitrogen-doped carbon nanospheres for supercapacitor application. First, when compared to the various carbon morphologies mentioned earlier, carbon spheres can be obtained simply by direct carbon conversion of polymer spheres made of phenolic resins or polystyrene.[21,22] The porosity of carbon spheres can be controlled by incorporating soft templates into the polymer spheres.[21] Moreover, control of the intracross-linking of polymer spheres provides a template-free approach to forming secondary pores around the carbon

Received: May 28, 2014
Accepted: July 22, 2014
Published: July 30, 2014

 © 2014 American Chemical Society dx.doi.org/10.1021/am5033378 | ACS Appl. Mater. Interfaces 2014, 6, 13968−13976

Scheme 1. (a) Procedure for the Synthesis of Nitrogen-Doped Carbon Nanospheres; (b) Cross-Linking Reaction of Styrenes via Friedel–Crafts Alkylation

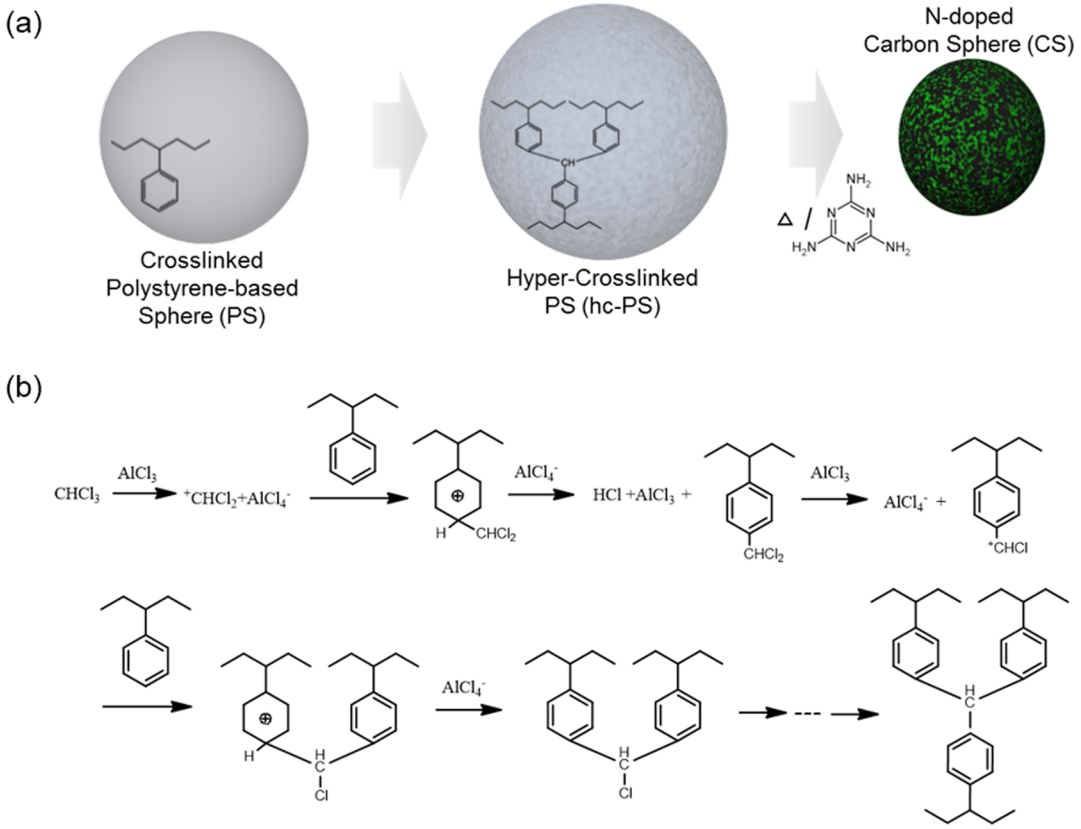

spheres.[22] However, few researchers have studied their performance in electrochemical applications and, to the best of our knowledge, there has been no report on doped carbon spheres for supercapacitors. In this study, pyrolytic carbonization with a nitrogen-enriched molecule, melamine (1,3,5-triazine-2,4,6-triamine), was utilized to obtain carbon spheres and simultaneous nitrogen doping. The doping content was controlled by the weight ratio of melamine to polymer spheres in the pyrolysis. The morphology of the nitrogen-doped carbon nanospheres, configuration of doped nitrogen, as well as carbon crystallinity was investigated. Our N-doped carbon sphere was also applied as an electrode material in supercapacitors. The remarkable capacitance of 192 F g^{-1} was obtained for 20% N-doped carbon nanospheres. Moreover, the capacitance retention remains up to 10 000 cycles, which clearly displays a good stability for the N-doped carbon nanospheres as supercapacitve electrode materials.

EXPERIMENTAL SECTION

Synthesis of Polystyrene-Based Spheres and Their Hyper-Cross-Linking. Monodispersed polystyrene-based polymer spheres (PS) were synthesized by emulsifier-free emulsion polymerization of styrene (99.9%, Aldrich) in deionized water. Methyl methacrylate monomer of 5 wt % (MMA, 98.5%, Aldrich) was added to control the size of the spheres. Briefly, the polymerization was carried out as follows: the styrene and the MMA in water were vigorously mixed along with 5 wt % (over the monomer weight) potassium persulfate (Aldrich). Then, 40 wt % (over the monomer weight) divinylbenzene (Aldrich) was added as a cross-linker. After the overnight polymerization, the polymer colloids were purified several times by centrifugal sedimentation and redispersion in deionized water. The hyper-cross-linking of the PS styrenes was achieved via Friedel–Crafts alkylation (see Figure S1 in the Supporting Information). The PS was dispersed in chloroform where 8 wt % of anhydrous aluminum chloride was dissolved, and the reaction was carried out at 60 °C for 8 h. The resulting hyper-cross-linked PS (hc-PS) was purified by washing with ethanol.

Carbonization and Nitrogen Doping. 1,3,5-Triazine-2,4,6-triamine, that is, melamine powder (99%, Aldrich) was used as a nitrogen source. The melamine powder was mixed with the dried hc-PS, and placed in a tube furnace. The sample was first heated to 300 °C for 20 min under an argon atmosphere, and the temperature was then increased to 700 °C for 80 min.

Characterization. The surface morphologies were determined by a field emission scanning electron microscope (FESEM, Hitachi, S-4700) and an energy-filtering transmission electron microscope (EFTEM, Carl Zeiss, LIBRA 120, 80 kV). Energy dispersive spectroscopy (EDS) elemental mapping was performed with high-resolution transmission electron microscopes (HRTEM, JEOL, JEM-2100F, 200 kV). X-ray photoelectron spectroscopy (XPS, Thermo Fisher Scientific, ESCALAB 250 XPS System) analysis using a monochromated Al Kα X-ray source ($h\nu$ = 1486.6 eV) at a chamber pressure of 1×10^{-10} Torr was performed for elemental analysis. Raman spectra were recorded using micro Raman spectroscopy (Tokyo instrument, Nanofinder) with an excitation wavelength of 487.55 nm.

Electrochemical Measurements. A beaker-type three-electrode system was used to measure the electrochemical properties of the sample. To prepare the CS and N-CS working electrodes, CS and N-CS were dispersed in a mixture of Nafion solution (Aldrich) and anhydrous ethanol (Daejung) by sonication. This solution was transferred onto a GCE and dried at 60 °C, and used as a working electrode. A platinum wire and a Ag/AgCl (3 M NaCl) electrode was used as a counter and reference electrode. A 1 M H_2SO_4 (Aldrich) solution was prepared as electrolyte. Cyclic voltammetry (CV) and galvanostatic charge–discharge cycles were measured with a

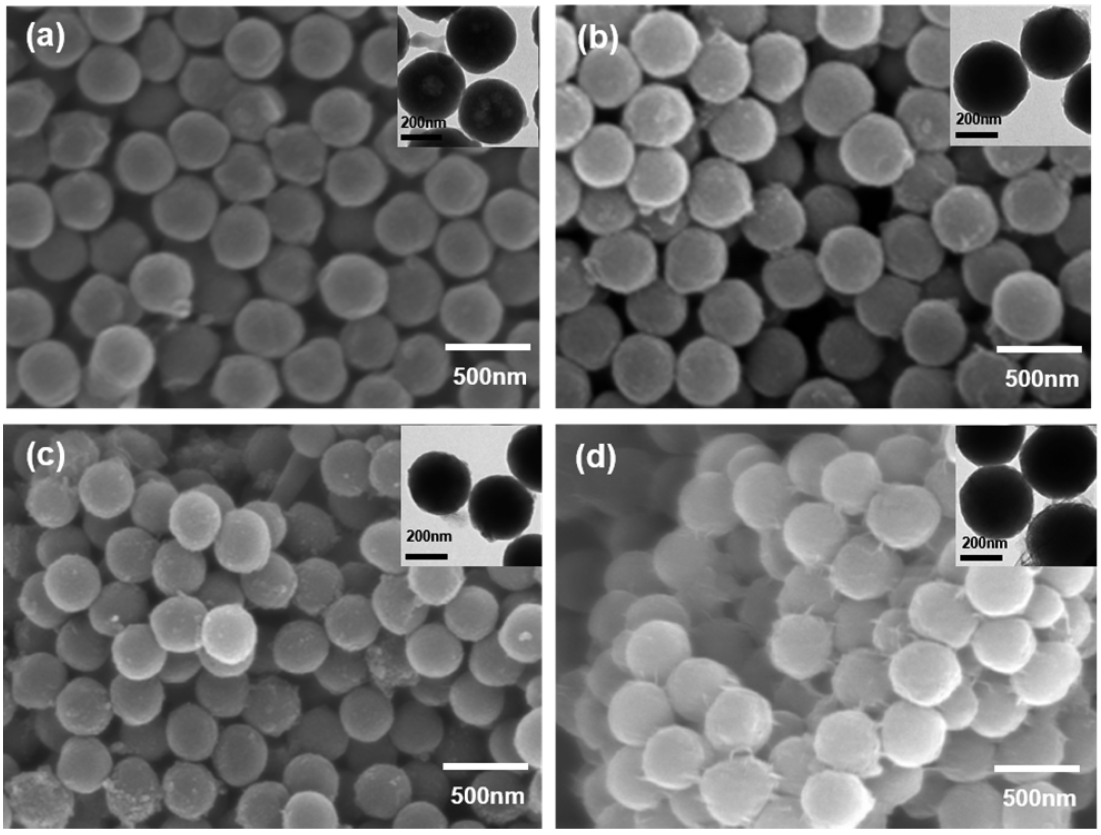

Figure 1. SEM images of (a) PS, (b) hc-PS, (c) low-N-CS, and (d) high-N-CS. The inset shows the TEM image of each sample.

VersaSTAT 3 (AMETEK) instrument. CV was performed with a potential window of 0−1 V versus a Ag/AgCl (3 M NaCl) electrode with a range of scan rates (from 5 to 200 mV s^{-1}). In the galvanostatic charge−discharge measurements, the cell was prepared with a voltage window of 0−1 V by applying a constant current of 0.1−1 A g^{-1}. The measurement was repeated at least three times and averaged to obtain the result.

RESULTS AND DISCUSSION

The preparation of size-monodispersed N-doped carbon nanospheres is illustrated in Scheme 1a. Briefly, a cross-linked polystyrene-based sphere was prepared, where the styrenes were further cross-linked via Friedel−Crafts alkylation as shown in Scheme 1b,[23] resulting in hyper-cross-linked polystyrene-based polymer spheres (hc-PS). The pyrolitic carbonization induced the reduction of hc-PS to carbon spheres. Here, the high-temperature pyrolysis of the hc-PS spheres with melamine (1,3,5-triazine-2,4,6-triamine) powder carbonized the hc-PS spheres, and simultaneously doped the nitrogen into the carbonized hc-PS.

Figure 1a and b shows the SEM images of monodispersed PS and hc-PS, respectively. The hyper-cross-linking is required to enhance polymer-to-carbon conversion.[24] Briefly, as described in Scheme 1b, the hyper-cross-linking of styrene groups was initiated by the formation of benzyl carbocation in the presence of a Friedel−Craft catalyst, $AlCl_3$, and proceeded by linking the benzyl chloromethyl carbocation with polystyrenes. The diameter of the PS and hc-PS spheres was 350 and 380 nm, respectively. We found that the particle size increased during the hyper-cross-linking, which may be attributed to the increase in free volume of polymer networks in the cross-linking reaction.[25] Meanwhile, Figure 1c and d shows SEM images of the PS-carbonized carbon sphere (CS) at 700 °C, in the presence of melamine during the carbonization. Previously, nitrogen doping has been achieved by chemical vapor deposition using ammonia and a pyridine precursor,[26] thermal treatment in an ammonia gas environment,[27] or using a nitrogen-enriched solid precursor such as melamine.[28,29] In comparison, the use of melamine was cost-effective and achieved a relatively high doping concentration. The following doping mechanism has been reported: in the temperature range of 300−600 °C, melamine is decomposed into carbon nitrides[30] (see Figure S2), and at a higher temperature nitrogen is released, which diffuses into the carbon matrix. Here, the doping concentration was controlled by setting the mixing weight ratio of hc-PS to melamine at 1:5 (Figure 1c) and 1:50 (Figure 1d). We designated the CS prepared with the 1:5 carbon/melamine weight ratio as low-N-CS, and the CS prepared with the 1:50 carbon/melamine weight ratio as high-N-CS. Figure 1c and d clearly show that the spherical shape was maintained during the pyrolytic carbonization. The diameters of the low-N-CS and high-N-CS were shrunk to be 310 and 355 nm, respectively; the size shrinkage was 18.5% and 6.6%, respectively. On the other hand, in the case of the undoped CS, the diameter was measured to be around 270 nm (i.e., 29.0% shrinkage), as shown Figure S3. Thus, we clearly observed that the extent of size shrinkage during carbonization was more greatly reduced by increasing the amount of N doping. This may be explained by the fact that nitrogen doping "swells" the CS, induces a loose packing of graphitic carbon crystallites. Pore characterization was achieved by Brunauer−Emmett−Teller (BET) adsorption/desorption measurements as shown in Figure S4 and Table S1. The results showed that the BET area of undoped CS, low-N-CS, and high-N-CS was 41.2, 93.7,

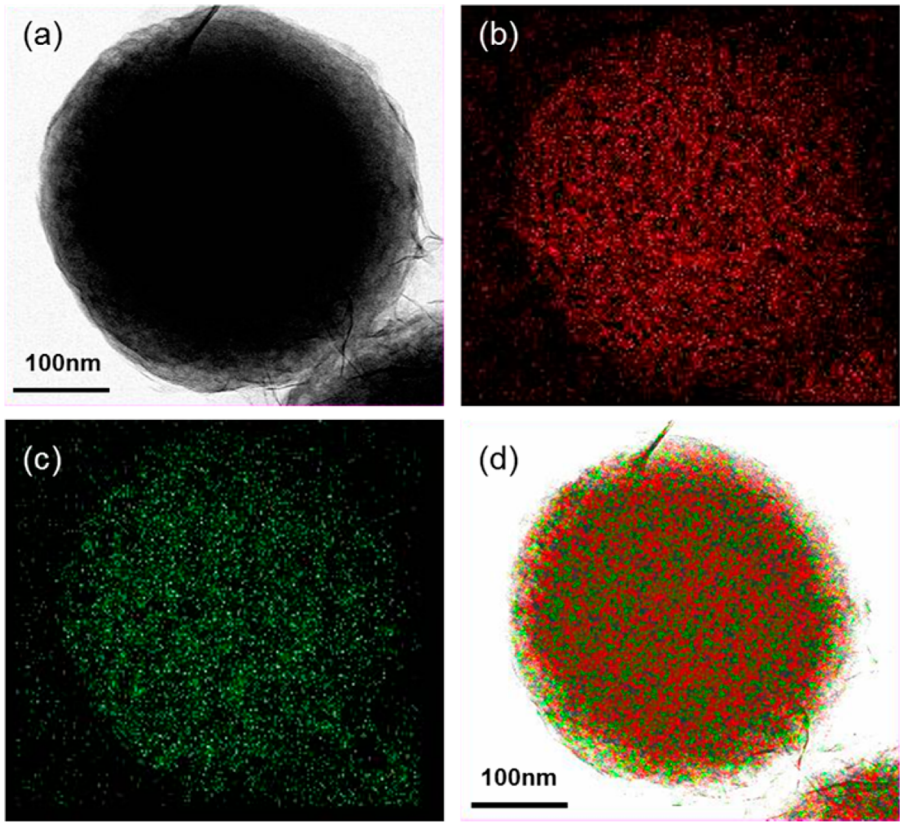

Figure 2. Scanning TEM (STEM) image of (a) high-N-CS and the elemental mapping images of (b) carbon, (c) nitrogen, and the (d) overlay of the STEM image and the elemental mapping images.

and 145.5 $m^2 g^{-1}$, respectively. The increase in specific surface area with increasing nitrogen doping was attributed to the increase in micropores observed at a low relative pressure range. This result also corresponds to the morphology change caused by the nitrogen doping.

Scanning TEM with elemental mapping was carried out to confirm the nitrogen doping in the carbon sphere and to characterize the doping uniformity. Figure 2a−c shows TEM images of a high-N-CS and its elemental mapping of carbon and nitrogen elements, respectively. Figure 2d is an overlay image of these images, and clearly shows that nitrogen is uniformly distributed in a spherical particle. The elemental composition and nitrogen bonding configurations of N-doped CS were further quantified by XPS measurements. The XPS survey spectrum is shown in Figure 3a, and a summary is listed in Table S2. The XPS results of undoped CS were also listed for comparison. The low-N-doped CS and high-N-doped CS showed a 2.50% and 21.6% nitrogen doping concentration, respectively, while the undoped CS showed no nitrogen content. The doping concentration was proportional to the mixing weight ratio. As for oxygen content, the concentration decreased with increasing nitrogen doping as shown in Table S2. The oxygenated group on the carbon surface has been known to mediate nitrogen doping; the nitrogen was thus preferably introduced at highly active sites in the carbon lattice e.g, dangling bonds produced by the oxygen detachment.[28,31] Thus, the high level of nitrogen doping accompanied by the low oxygen content in the N-CS implies that the oxygen groups incorporated into the CS were involved in the nitrogen doping.

The bonding configurations of the nitrogen atoms were characterized by high resolution N 1s spectra. Figure 3b and c shows N 1s spectra for low-N-CS and high-N-CS, respectively. The spectra were deconvoluted by four peaks at 398.2−398.6, 399.5−399.7, 400.7−400.8, and 402.5−402.6 eV. The peaks with low binding energy were attributed to pyridinic nitrogen, where the N atom has a sp^2 hybridization with two C atoms (N-6), and to pyrrolic nitrogen, where the N atom is incorporated into a five-membered ring of C atoms (N-5).[32,33] The peak at 400.7−400.8 eV designates quaternary nitrogen (N-Q), which substitutes carbon atoms in a graphene layer and is therefore sp^3 hybridized with three C atoms.[34,35] The peak at 402.5−402.6 eV was attributed to pyridine oxide or the oxidized nitrogen (N-X) group.[36] In Figure 3d, the relative content of these nitrogen configurations in low-N-CS and high-N-CS was compared. The N-doped CS possesses a relatively high portion of the N-6 and N-5 configurations, and a low content of the N-Q configuration. With high N doping, the N-Q configuration is reduced, while the N-6 and N-5 configurations are increased. Previous studies investigating the effect of annealing temperature or time on the configuration of doped nitrogen have revealed that a higher temperature or a longer period of treatment favored the N-Q configuration over the others.[17,34,37] The theoretical analysis also confirmed that higher energy is required to form the N-Q configuration.[38] Thus, it is reasonable to observe that nitrogen configurations other than N-Q were produced in greater extent when the nitrogen doping content was increased. Meanwhile, it has been reported that the N-5 and N-6 configurations induced the pseudocapacitance enhancement while the N-Q configuration improves the conductivity of carbon materials.[19,20]

The effect of nitrogen doping on the carbon micro-crystallinity of CS was investigated by Raman spectroscopy.

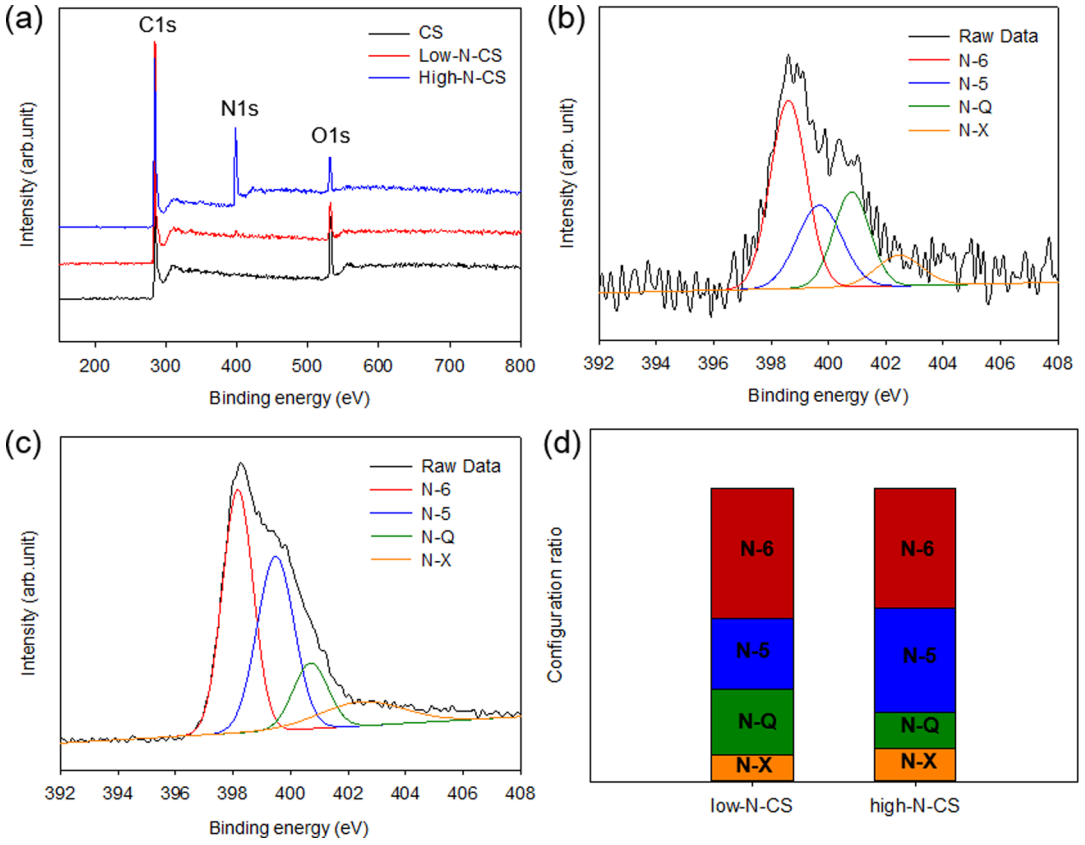

Figure 3. XPS survey spectrum of (a) undoped CS, low-N-CS, and high-N-CS. High resolution N 1s XPS spectra of (b) low-N-CS, (c) high-N-CS, and (d) their corresponding nitrogen configuration ratio.

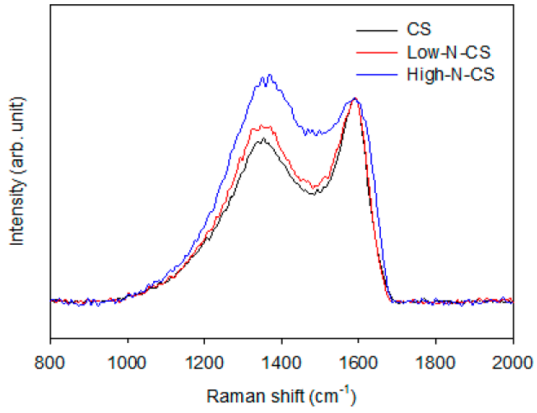

Figure 4. Raman spectra of the undoped CS, low-N-CS, and high-N-CS.

Figure 4 shows the Raman spectra of undoped CS, low-N-CS, and high-N-CS. In the figure, peaks centered at around 1347 and 1585 cm^{-1} were observed, which correspond, respectively, to the D-band caused by structural defects and the partially disordered structure of sp^2 domains, and the G-band associated with the first-order scattering of the E_{2g} vibrations observed for sp^2 domains.[39] The Raman spectra of the undoped CS displayed a D band at 1347 cm^{-1} and a G-band at 1581 cm^{-1}. The low-N-CS and high-N-CS displayed D and G bands at 1347 cm^{-1} and around 1590 cm^{-1}, respectively. The G-band of N-doped CS shifts toward a higher wavenumber.[40] Moreover, by increasing the nitrogen doping concentration, an increase in the D band is observed. This implies that structural defects and edge plane exposure were increased by increasing the nitrogen incorporation. Qualitatively, the peak intensity ratio between the D and G bands (I_D/I_G) inversely depends on the in-plane crystallite size L_a, which can be described by the Tuinstra–Koenig relationship:

$$L_a = (2.4 \times 10^{-10})\lambda^4 (I_D/I_G)^{-1}$$

where λ is the excitation wavelength. The I_D/I_G of the undoped CS, low-N-CS, and high-N-CS was 0.8080, 0.8737, and 1.1251, respectively.[41] The corresponding L_a values of the undoped CS, low-N-CS, and high-N-CS from the above equation were 16.78, 15.52, and 12.05 nm, respectively, which confirms an increase in disorder in the microcrystalline carbon due to the N doping.[42] This result may support the swelling of CS by the nitrogen doping as mentioned above.

We then prepared an electrode film by assembling the as-synthesized undoped CS or N-doped CS. The undoped CS and N-doped CS were dispersed in an ethanol solution and casted to be used as a working electrode. First, we investigated the effect of nitrogen doping on the electrochemical properties using cyclic voltammetry (CV) measurements. The CV was measured in a 1 M H_2SO_4 electrolyte solution. Figure 5a–c shows the CV curves measured at various scan rates for the undoped CS, low-N-CS, and high-N-CS, respectively. The undoped CS sample showed a redox peak, which is the result of the quinone/hydroquinone reaction of surface oxygenated groups.[43] On increasing the nitrogen doping concentration, the redox peak in the CV curve became less pronounced, while a redox hump was observed at a higher potential. Previously, the nitrogen-doped carbon had often shown no prominent redox peak in the CV curve, but had instead shown a redox hump,

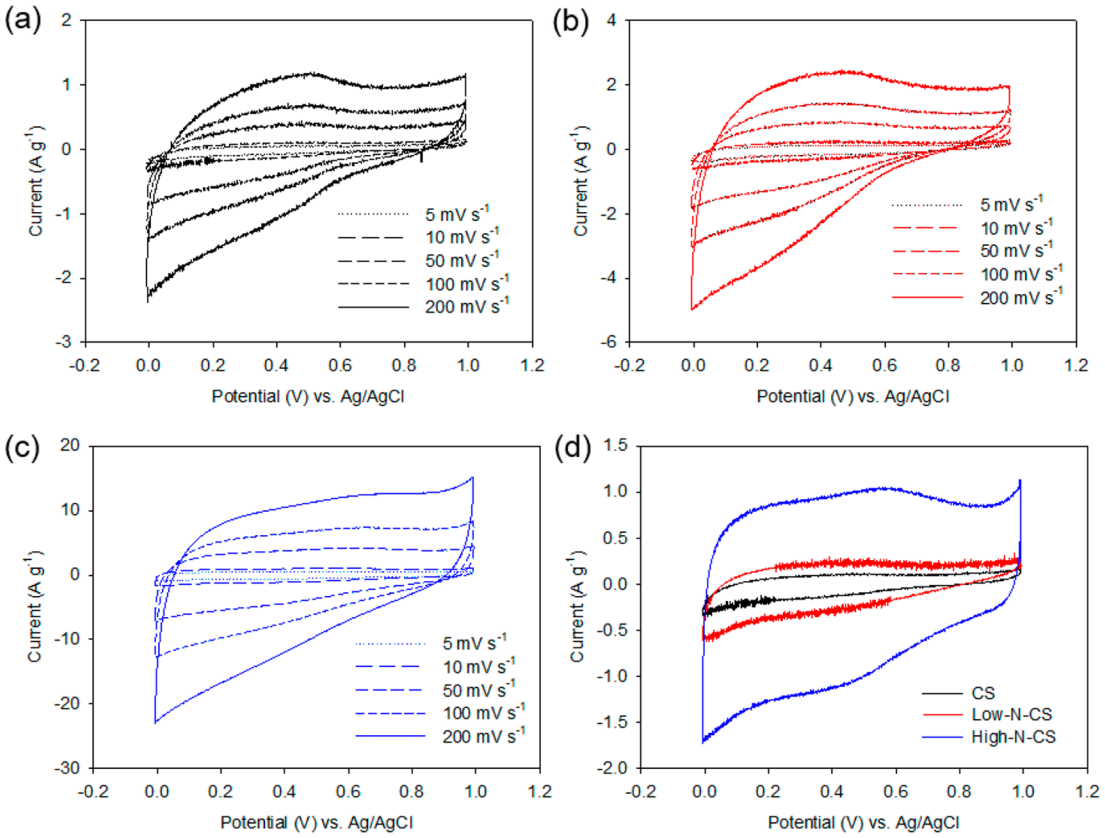

Figure 5. CV curves for the (a) undoped CS, (b) low-N-CS, and (c) high-N-CS at different scan rates. (d) CV curves for the undoped CS, low-N-CS, and high-N-CS at a scan rate of 10 mV s^{-1}. A 1 M H_2SO_4 solution was used as the electrolyte solution.

which corresponds to redox reactions at different sites, including doped nitrogen or the carbon adjacent to the nitrogen atom.[44] Figure 5d compares the CV curves of these samples at a scan rate of 10 mV s^{-1}. Due to the higher nitrogen doping, the area under the CV curve was larger, which indicates a higher electrochemical capacitive property in the N-doped CS sample. The enhancement of the electrochemical capacitive properties of N-doped CS may be attributed to pseudocapacitance by the nitrogen functionalities. This also indicates a lesser effect arising from the increase in specific surface area caused by nitrogen doping. Meanwhile, the enhancement of pseudocapacitance may be supported by the presence of the N-6 and N-5 doping of N-doped CS sample in the XPS analysis.

The galvanostatic charge/discharge measurement was taken and analyzed to characterize C_s performance (i.e., the specific capacitance) as applied in supercapacitors. It is reported that the galvanostatic charge/discharge measurement predict the pseudocapacitance more accurately. Figure 6a−c shows the galvanostatic charge/discharge curve at various current densities (0.1−1 A g^{-1}) for undoped CS, low-N-CS, and high-N-CS, respectively. First, in the discharge curve, the ohmic voltage drop was observed, which corresponds to the resistance of the electrode; the voltage drops for undoped CS, low-N-CS, and high-N-CS were 0.144, 0.100, and 0.012 V, respectively, at 0.1 A g^{-1}. These results show that higher nitrogen doping decreased the resistance of carbon materials. It has been reported that nitrogen doping enhanced the electrical conductivity and electrolyte solution wettability of the carbon materials, and thereby enhanced the capacitance.[13,15] Figure 6d compares the charge/discharge curve of undoped CS, low-N-CS, and high-N-CS at a current density of 0.1 A g^{-1}. Here, the specific capacitances of all the samples were calculated from the charge/discharge curve according to the following equation:[45]

$$C_s = It/(\Delta Vm)$$

where C_s is the specific capacitance, I is the discharge current, Δt is the discharge time, ΔV is the voltage range, and m is the mass of active materials on the electrode. The specific capacitance of the undoped CS, low-N-CS, and high-N-CS was calculated to be 13.44, 42.74, and 191.91 F g^{-1}, respectively. Compared to the undoped CS, the low-N-CS and high-N-CS enhanced the specific capacitance by 3.2 times and 14 times, respectively. This remarkable increase in the specific capacitance was attributed to the enhancement of pseudocapacitance by nitrogen functionalities and the electric conductivity of the carbon materials. The specific capacitance of the high-N-CS is comparable to the values of recently studied N-doped carbon nanofibers,[17] graphenes,[46] and mesoporous carbons.[16] The durability of the N-CS electrode was evaluated by the long-term charge/discharge behavior. Figure 7 displays the capacitance of the high-N-CS and the as a function of cycle number at a current density of 1 A g^{-1}. The capacitance retention remains at approximately within 110% at 10 000 cycles, which clearly displays a good cycling stability of high-N-CS as the supercapacitve electrode materials.

CONCLUSION

A direct carbonization with nitrogen-enriched melamine has been demonstrated to synthesize highly monodispersed nitrogen-doped carbon nanospheres with submicrometer sizes. We have controlled the nitrogen content of the doped nanospheres by adjusting the weight ratio of melamine to

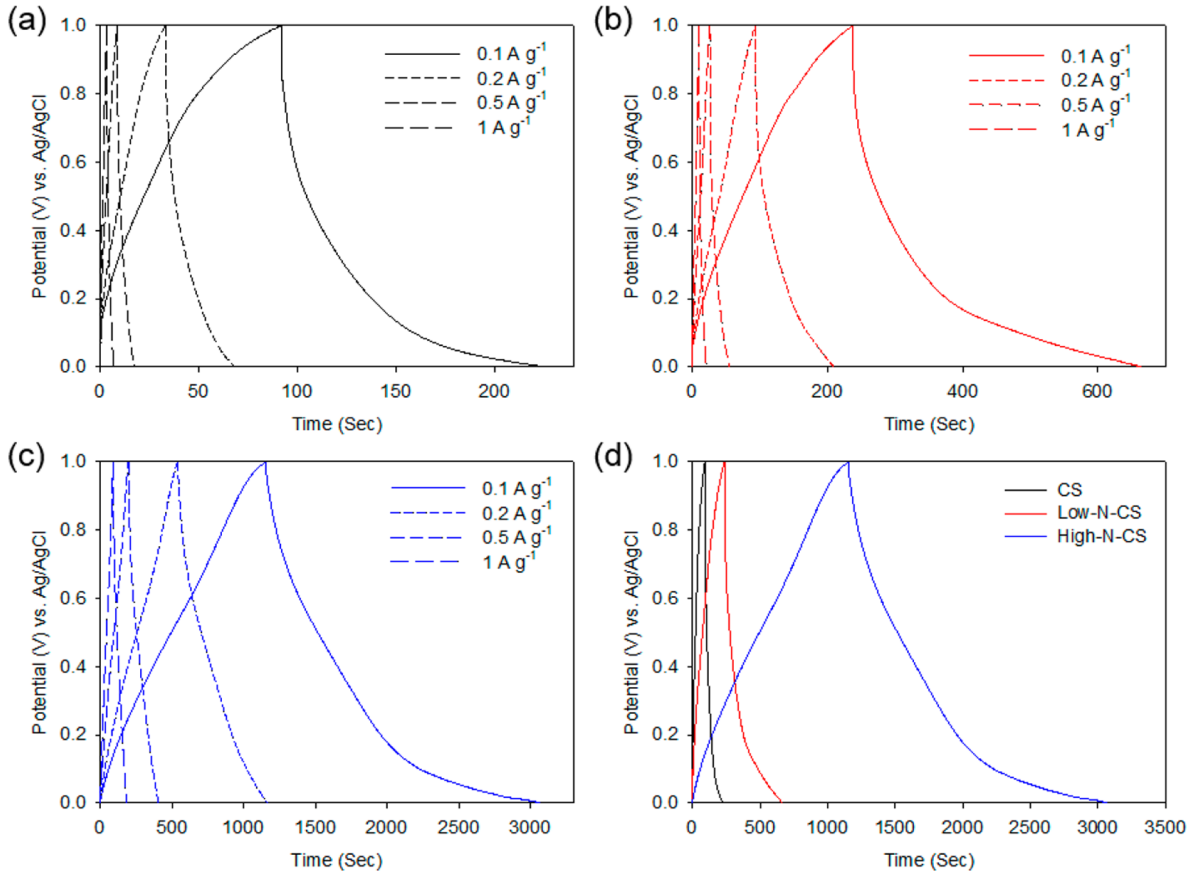

Figure 6. Galvanostatic charge−discharge curves for the (a) undoped CS, (b) low-N-CS, and (c) high-N-CS at different current densities. (d) Galvanostatic charge−discharge curve of the undoped CS, low-N-CS, and high-N-CS at a current density of 0.1 A g^{-1}.

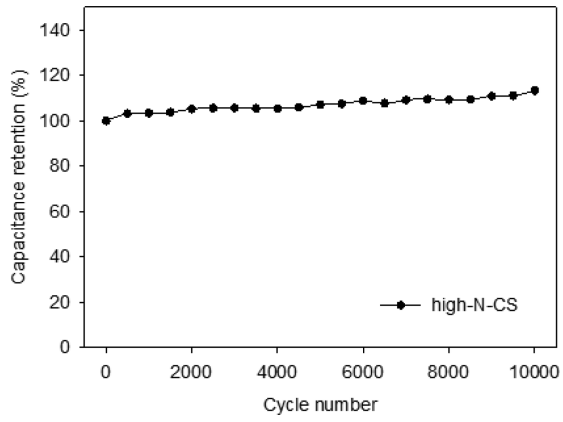

Figure 7. Capacitance retention of the high-N-CS measured at a constant current density of 1 A g^{-1}.

hyper-cross-linked polystyrene-based polymer spheres in the carbonization process. The doping was increased in proportion to this ratio, resulting in nitrogen doping of up to 20%. Pyrolytic carbonization of the polymer spheres caused their volume to shrink by up to 65%, while it was observed that nitrogen doping induced less shrinkage. Low and high doping contents led to 49.0% and 21.9% shrinkage, respectively, due to nitrogen addition, which causes the carbon matrix to swell and subsequently disintegrates the carbon crystallinity. The nitrogen doping produced relatively abundant pyridinic and pyrrolic configurations, which possess lower binding energies than quaternary nitrogen and oxidized nitrogen. These pyridinic and pyrrolic configurations were observed to be more abundant for carbon nanospheres with high nitrogen doping. The nitrogen-doped carbon spheres were then assembled for use as electrodes in electrochemical supercapacitors. The nitrogen doping enhanced the pseudocapacitance and the electrical conductivity of carbon, thereby enhancing the specific capacitance. We obtained a capacitance of up to 191.9 F g^{-1} with 20% nitrogen doped carbon nanospheres, which was 14 times higher than that of the undoped carbon nanospheres. Moreover, the nitrogen-doped carbon nanospheres showed a good cycling stability up to 10 000 cycles. We believe that engineering of the particle porosity or the self-assembled packing of carbon nanospheres may further enhance the supercapacitance properties.

■ ASSOCIATED CONTENT

Supporting Information

FT-IR spectra of PS and hc-PS. TEM images of partially carbonized PS spheres with and without melamine. SEM, XPS images of the undoped CS. BET, XPS, and EDX analysis of the CS and N-doped CS. This material is available free of charge via the Internet at http://pubs.acs.org.

■ AUTHOR INFORMATION

Corresponding Author

*E-mail: junhyuk@sogang.ac.kr.

Notes

The authors declare no competing financial interest.

■ ACKNOWLEDGMENTS

This work was supported by grants from the National Research Foundation of Korea (2012M1A2A2671794, 2013R1A1A2010973). The Korea Basic Science Institute is also acknowledged for the SEM measurements.

■ REFERENCES

(1) Gao, W.; Singh, N.; Song, L.; Liu, Z.; Reddy, A. L. M.; Ci, L.; Vajtai, R.; Zhang, Q.; Wei, B.; Ajayan, P. M. Direct Laser Writing of Micro-Supercapacitors on Hydrated Graphite Oxide Films. *Nat. Nanotechnol.* **2011**, *6*, 496−500.

(2) Pech, D.; Brunet, M.; Durou, H.; Huang, P.; Mochalin, V.; Gogotsi, Y.; Taberna, P.-L.; Simon, P. Ultrahigh-Power Micrometre-Sized Supercapacitors Based on Onion-Like Carbon. *Nat. Nanotechnol.* **2010**, *5*, 651−654.

(3) Conway, B. *Electrochemical Supercapacitors: Scientific Fundamentals and Technological Applications (Pod)*; Kluwer Academic/Plenum: New York, 1999.

(4) Zhai, Y.; Dou, Y.; Zhao, D.; Fulvio, P. F.; Mayes, R. T.; Dai, S. Carbon Materials for Chemical Capacitive Energy Storage. *Adv. Mater.* **2011**, *23*, 4828−4850.

(5) Du, F.; Yu, D.; Dai, L.; Ganguli, S.; Varshney, V.; Roy, A. K. Preparation of Tunable 3d Pillared Carbon Nanotube−Graphene Networks for High-Performance Capacitance. *Chem. Mater.* **2011**, *23*, 4810−4816.

(6) Luo, G.; Liu, L.; Zhang, J.; Li, G.; Wang, B.; Zhao, J. Hole Defects and Nitrogen Doping in Graphene: Implication for Supercapacitor Applications. *ACS Appl. Mater. Interfaces* **2013**, *5*, 11184−11193.

(7) Horike, S.; Umeyama, D.; Kitagawa, S. Ion Conductivity and Transport by Porous Coordination Polymers and Metal-Organic Frameworks. *Acc. Chem. Res.* **2013**, *46*, 2376−2384.

(8) Fuertes, A. B.; Pico, F.; Rojo, J. M. Influence of Pore Structure on Electric Double-Layer Capacitance of Template Mesoporous Carbons. *J. Power Sources* **2004**, *133*, 329−336.

(9) Mastragostino, M.; Arbizzani, C.; Soavi, F. Conducting Polymers as Electrode Materials in Supercapacitors. *Solid State Ionics* **2002**, *148*, 493−498.

(10) Gund, G. S.; Dubal, D. P.; Shinde, S. S.; Lokhande, C. D. Architectured Morphologies of Chemically Prepared Nio/Mwcnts Nanohybrid Thin Films for High Performance Supercapacitors. *ACS Appl. Mater. Interfaces* **2014**, *6*, 3176−3188.

(11) Wu, N.-L. Nanocrystalline Oxide Supercapacitors. *Mater. Chem. Phys.* **2002**, *75*, 6−11.

(12) Xu, D.; Xu, Q.; Wang, K.; Chen, J.; Chen, Z. Fabrication of Free-Standing Hierarchical Carbon Nanofiber/Graphene Oxide/Polyaniline Films for Supercapacitors. *ACS Appl. Mater. Interfaces* **2014**, *6*, 200−209.

(13) Lee, Y.-H.; Lee, Y.-F.; Chang, K.-H.; Hu, C.-C. Synthesis of N-Doped Carbon Nanosheets from Collagen for Electrochemical Energy Storage/Conversion Systems. *Electrochem. Commun.* **2011**, *13*, 50−53.

(14) Vagner, C.; Finqueneisel, G.; Zimny, T.; Burg, P.; Grzyb, B.; Machnikowski, J.; Weber, J. V. Characterization of the Surface Properties of Nitrogen-Enriched Carbons by Inverse Gas Chromatography Methods. *Carbon* **2003**, *41*, 2847−2853.

(15) Guo, H.; Gao, Q. Boron and Nitrogen Co-Doped Porous Carbon and Its Enhanced Properties as Supercapacitor. *J. Power Sources* **2009**, *186*, 551−556.

(16) Frackowiak, E.; Lota, G.; Machnikowski, J.; Vix-Guterl, C.; Béguin, F. Optimisation of Supercapacitors Using Carbons with Controlled Nanotexture and Nitrogen Content. *Electrochim. Acta* **2006**, *51*, 2209−2214.

(17) Chen, L.-F.; Zhang, X.-D.; Liang, H.-W.; Kong, M.; Guan, Q.-F.; Chen, P.; Wu, Z.-Y.; Yu, S.-H. Synthesis of Nitrogen-Doped Porous Carbon Nanofibers as an Efficient Electrode Material for Supercapacitors. *ACS Nano* **2012**, *6*, 7092−7102.

(18) Béguin, F.; Szostak, K.; Lota, G.; Frackowiak, E. A Self-Supporting Electrode for Supercapacitors Prepared by One-Step Pyrolysis of Carbon Nanotube/Polyacrylonitrile Blends. *Adv. Mater.* **2005**, *17*, 2380−2384.

(19) Tan, Y.; Xu, C.; Chen, G.; Liu, Z.; Ma, M.; Xie, Q.; Zheng, N.; Yao, S. Synthesis of Ultrathin Nitrogen-Doped Graphitic Carbon Nanocages as Advanced Electrode Materials for Supercapacitor. *ACS Appl. Mater. Interfaces* **2013**, *5*, 2241−2248.

(20) Yang, X.; Wu, D.; Chen, X.; Fu, R. Nitrogen-Enriched Nanocarbons with a 3-D Continuous Mesopore Structure from Polyacrylonitrile for Supercapacitor Application. *J. Mater. Chem. A* **2010**, *114*, 8581−8586.

(21) Wang, D.-W.; Li, F.; Liu, M.; Lu, G. Q.; Cheng, H.-M. 3D Aperiodic Hierarchical Porous Graphitic Carbon Material for High-Rate Electrochemical Capacitive Energy Storage. *Ang. Chem., Int. Ed.* **2008**, *47*, 373−376.

(22) Lee, J.; Kim, J.; Hyeon, T. Recent Progress in the Synthesis of Porous Carbon Materials. *Adv. Mater.* **2006**, *18*, 2073−2094.

(23) Jordan, D. O.; Mathieson, A. R. 111. The Kinetics of Catalytic Polymerizations. Part I. The Polymerization of Styrene Catalyzed by Aluminium Chloride in Carbon Tetrachloride Solution. *J. Chem. Soc.* **1952**, 611−620.

(24) Bussing, W. R.; Peppas, N. A. Friedel-Crafts Crosslinking Methods for Polystyrene Modification: 1. Preparation and Kinetics. *Polymer* **1983**, *24*, 209−216.

(25) Davankov, V. A.; Pastukhov, A. V.; Tsyurupa, M. P. Unusual Mobility of Hypercrosslinked Polystyrene Networks: Swelling and Dilatometric Studies. *J. Polym. Sci., Part B: Polym. Phys.* **2000**, *38*, 1553−1563.

(26) Panchakarla, L. S.; Subrahmanyam, K. S.; Saha, S. K.; Govindaraj, A.; Krishnamurthy, H. R.; Waghmare, U. V.; Rao, C. N. R. Synthesis, Structure, and Properties of Boron- and Nitrogen-Doped Graphene. *Adv. Mater.* **2009**, *21*, 4726−4730.

(27) Wang, X.; Li, X.; Zhang, L.; Yoon, Y.; Weber, P. K.; Wang, H.; Guo, J.; Dai, H. N-Doping of Graphene through Electrothermal Reactions with Ammonia. *Science* **2009**, *324*, 768−771.

(28) Sheng, Z.-H.; Shao, L.; Chen, J.-J.; Bao, W.-J.; Wang, F.-B.; Xia, X.-H. Catalyst-Free Synthesis of Nitrogen-Doped Graphene Via Thermal Annealing Graphite Oxide with Melamine and Its Excellent Electrocatalysis. *ACS Nano* **2011**, *5*, 4350−4358.

(29) Lin, Z.; Song, M.-k.; Ding, Y.; Liu, Y.; Liu, M.; Wong, C.-p. Facile Preparation of Nitrogen-Doped Graphene as a Metal-Free Catalyst for Oxygen Reduction Reaction. *Phys. Chem. Chem. Phys.* **2012**, *14*, 3381−3387.

(30) Groenewolt, M.; Antonietti, M. Synthesis of g-C_3N_4 Nanoparticles in Mesoporous Silica Host Matrices. *Adv. Mater.* **2005**, *17*, 1789−1792.

(31) Li, X.; Wang, H.; Robinson, J. T.; Sanchez, H.; Diankov, G.; Dai, H. Simultaneous Nitrogen Doping and Reduction of Graphene Oxide. *J. Am. Chem. Soc.* **2009**, *131*, 15939−15944.

(32) Shrestha, S.; Mustain, W. E. Properties of Nitrogen-Functionalized Ordered Mesoporous Carbon Prepared Using Polypyrrole Precursor. *J. Electrochem. Soc.* **2010**, *157*, B1665−B1672.

(33) Kapteijn, F.; Moulijn, J. A.; Matzner, S.; Boehm, H. P. The Development of Nitrogen Functionality in Model Chars During Gasification in CO_2 and O_2. *Carbon* **1999**, *37*, 1143−1150.

(34) Su, F.; Poh, C. K.; Chen, J. S.; Xu, G.; Wang, D.; Li, Q.; Lin, J.; Lou, X. W. Nitrogen-Containing Microporous Carbon Nanospheres with Improved Capacitive Properties. *Energy Environ. Sci.* **2011**, *4*, 717−724.

(35) Hulicova-Jurcakova, D.; Kodama, M.; Shiraishi, S.; Hatori, H.; Zhu, Z. H.; Lu, G. Q. Nitrogen-Enriched Nonporous Carbon Electrodes with Extraordinary Supercapacitance. *Adv. Funct. Mater.* **2009**, *19*, 1800−1809.

(36) Xu, F.; Minniti, M.; Barone, P.; Sindona, A.; Bonanno, A.; Oliva, A. Nitrogen Doping of Single Walled Carbon Nanotubes by Low Energy Ion Implantation. *Carbon* **2008**, *46*, 1489−1496.

(37) Van Khai, T.; Na, H. G.; Kwak, D. S.; Kwon, Y. J.; Ham, H.; Shim, K. B.; Kim, H. W. Significant Enhancement of Blue Emission and Electrical Conductivity of N-Doped Graphene. *J. Mater. Chem.* **2012**, *22*, 17992−18003.

(38) Wang, D.-W.; Li, F.; Yin, L.-C.; Lu, X.; Chen, Z.-G.; Gentle, I. R.; Lu, G. Q.; Cheng, H.-M. Nitrogen-Doped Carbon Monolith for Alkaline Supercapacitors and Understanding Nitrogen-Induced Redox Transitions. *Chem.—Eur. J.* **2012**, *18*, 5345−5351.
(39) Kudin, K. N.; Ozbas, B.; Schniepp, H. C.; Prud'homme, R. K.; Aksay, I. A.; Car, R. Raman Spectra of Graphite Oxide and Functionalized Graphene Sheets. *Nano Lett.* **2007**, *8*, 36−41.
(40) Yang, X.; Li, C.; Wang, W.; Yang, B.; Zhang, S.; Qian, Y. A Chemical Route from Ptfe to Amorphous Carbon Nanospheres in Supercritical Water. *Chem. Commun.* **2004**, 342−343.
(41) Cançado, L. G.; Takai, K.; Enoki, T.; Endo, M.; Kim, Y. A.; Mizusaki, H.; Jorio, A.; Coelho, L. N.; Magalhães-Paniago, R.; Pimenta, M. A. General Equation for the Determination of the Crystallite Size L_a of Nanographite by Raman Spectroscopy. *Appl. Phys. Lett.* **2006**, *88*, 163106.
(42) Zhang, C.; Fu, L.; Liu, N.; Liu, M.; Wang, Y.; Liu, Z. Synthesis of Nitrogen-Doped Graphene Using Embedded Carbon and Nitrogen Sources. *Adv. Mater.* **2011**, *23*, 1020−1024.
(43) Senthilkumar, S. T.; Senthilkumar, B.; Balaji, S.; Sanjeeviraja, C.; Kalai Selvan, R. Preparation of Activated Carbon from Sorghum Pith and Its Structural and Electrochemical Properties. *Mater. Res. Bull.* **2011**, *46*, 413−419.
(44) Ouyang, Y.; Shi, H.; Fu, R.; Wu, D. Highly Monodisperse Microporous Polymeric and Carbonaceous Nanospheres with Multifunctional Properties. *Sci. Rep.* **2013**, *3*, 1430.
(45) Zhao, L.; Fan, L.-Z.; Zhou, M.-Q.; Guan, H.; Qiao, S.; Antonietti, M.; Titirici, M.-M. Nitrogen-Containing Hydrothermal Carbons with Superior Performance in Supercapacitors. *Adv. Mater.* **2010**, *22*, 5202−5206.
(46) Hassan, F. M.; Chabot, V.; Li, J.; Kim, B. K.; Ricardez-Sandoval, L.; Yu, A. Pyrrolic-Structure Enriched Nitrogen Doped Graphene for Highly Efficient Next Generation Supercapacitors. *J. Mater. Chem.* **2013**, *1*, 2904−2912.